n-type doping and passivation of $CuInSe_2$ and $CuGaSe_2$ by hydrogen

Çetin Kılıç and Alex Zunger
National Renewable Energy Laboratory, Golden, Colorado 80401, USA
(Received 28 March 2003; revised manuscript received 8 April 2003; published 7 August 2003)

An impurity in a semiconductor can have either amphoteric behavior (no net production of electron or holes), or be an energetically deep center (carriers produced only at high temperature), or a shallow center (carriers produced even at low temperature). In most semiconductors (e.g., Si, GaAs, GaP, InP, and ZnSe) hydrogen impurities do not produce free carriers, being instead an amphoretic center; yet hydrogen does dope *n*-type some oxides such as SnO_2 and ZnO. We studied theoretically whether or not H could dope chalcopyrite I-III-VI_2 compounds, $CuInSe_2$ and $CuGaSe_2$. Based on the first-principles calculations, we find that nonsubstitutionally incorporated hydrogen forms a *deep* donor in $CuGaSe_2$, but a *relatively shallow* donor in $CuInSe_2$. The interaction of hydrogen with the abundant defect complex $(2V_{Cu}+In_{Cu})^0$ yields an even *shallower* donor, making $CuInSe_2$ *n* type. In addition, our results show that hydrogen passivates the acceptorlike copper vacancies in both $CuInSe_2$ and $CuGaSe_2$, thus eliminating *p* type behavior. These findings, in conjunction with typical conditions under which $CuInSe_2$ and $CuGaSe_2$ are grown, indicate that $CuInSe_2$ could be doped *n* type via hydrogen incorporation, whereas $CuGaSe_2$ could not. The reason for the different behavior of $CuInSe_2$ and $CuGaSe_2$ towards hydrogen is that in the latter case the conduction-band minimum is at a considerably higher energy than in the former case. Despite this difference in electrical properties, it is predicted that hydrogen can be stored in both $CuInSe_2$ and $CuGaSe_2$ via implantation since the implanted hydrogens decorate copper atoms as well as preexisting copper vacancies.

DOI: 10.1103/PhysRevB.68.075201 PACS number(s): 61.72.Ww, 71.55.Ht, 61.72.Ji, 61.72.Bb

I. INTRODUCTION

Hydrogen is a ubiquitous impurity in many semiconductors,[1] but its incorporation as an electrical dopant is rare, since it normally acts to passivate existing carriers, forming an acceptor level in *n*-type and a donor level in *p*-type materials, e.g., in Si (Ref. 2), GaAs (Ref. 3), GaP (Ref. 4), InP (Ref. 5), and ZnSe (Ref. 6). We have recently shown,[7] however, that hydrogen in *n*-type SnO_2 (Ref. 8) forms a shallow donor, enhancing *n*-type electrical conduction. Furthermore, we predicted[7] *n*-type dopability by H of some large electron-affinity oxides such as TiO_2 and WO_3. Here, we enquire if hydrogen could be a potential candidate for *n*-type doping of chalcopyrites, i.e., I-III-VI_2 compounds. Indeed, it has already been demonstrated[9,10] that hydrogen implantation causes p-to-n conductivity-type conversion in $CuInSe_2$. Chalcopyrites used in solar cell applications are mostly being doped through stoichiometry control[11,12] (e.g., Cu deficiency leads to *p*-type acceptors) as opposed to chemical doping.[13] Such nonstoichiometric chalcopyrite samples, on the other hand, are highly compensated since they are rich in both intrinsic donors and acceptors.[14] Thus, doping by hydrogen could provide a better means when the current methods are unsatisfactory. Our results indicate that hydrogen incorporation could help for this purpose. We find, based on first-principles calculations, that nonsubstitutionally incorporated hydrogen forms a deep donor in $CuGaSe_2$, but a relatively shallow donor in $CuInSe_2$. The interaction of hydrogen with the abundant defect complex,[15] formed by pairing of indium antisite with two copper vacancies in compensated (i.e., nonstoichiometric) $CuInSe_2$, results in an even shallower donor, promising to make $CuInSe_2$ *n* type. Our results also reveal that hydrogen passivates the acceptor-like copper vacancies in both $CuInSe_2$ and $CuGaSe_2$, hence eliminating *p* type behavior. Thus, hydrogen incorporation could provide a novel means for *n*-type doping of $CuInSe_2$, and passivates acceptorlike defects in *p*-type $CuInSe_2$ and $CuGaSe_2$. In addition, we will show that under appropriate conditions, a copper vacancy in $Cu(In,Ga)Se_2$ could store as many as four hydrogen molecules.

II. METHOD OF CALCULATION

We calculate the defect transition energies to study the effect of hydrogen on the electrical properties of $Cu(In,Ga)Se_2$. The transition energy that corresponds to switching the charge state from q_1 to q_2 of defect D is given by

$$E_D(q_1/q_2)=\frac{E_D^{(q_2)}-E_D^{(q_1)}}{q_1-q_2}, \qquad (1)$$

where $E_D^{(q_i)}$ denotes the total energy for defect D in charge state q_i $(i=1,2)$ embedded in the host system $S=CuInSe_2$ or $CuGaSe_2$. If the Fermi energy E_F is smaller (larger) than $E_D(q_1/q_2)$, then the charge state of D is q_1 (q_2). Thus, $E_D(q_1/q_2)$ corresponds to the value of E_F at which the transition from charge state q_1 to q_2 takes place. The transition energy $E_D(q_1/q_2)$ could also be obtained from the defect formation energy of D in charge state q given by

$$\Delta H_D^{(q)}=[E_D^{(q)}-E_S]+\sum_\alpha n_\alpha(\mu_\alpha+\mu_\alpha^0) - n_H(\mu_H+\mu_H^0)+q(E_F+E_v), \qquad (2)$$

 ©2003 The American Physical Society

where E_S is the total energy of the pure host crystal S. The value of $\Delta H_D^{(q)}$ provides further an indication of whether or not the defect $D^{(q)}$ is stable, and thus, abundant. In Eq. (2), the first term denotes the change in total energy due to breaking host bonds and forming defect bonds; the second and third terms denote the change in chemical potential due to exchange of atoms between the host system and the atomic reservoirs of the elemental solids $\alpha=$Cu, In or Ga, and Se, and due to incorporation of hydrogen, respectively. n_α is then the number of atoms transferred to the atomic reservoir α, and $n_{\rm H}$ is the number of hydrogens incorporated; μ_α and $\mu_{\rm H}$ denote the respective atomic chemical potential with μ_α^0 being the zero of μ_α. The last term denotes the energy change owing to exchange of carriers between the defect and the Fermi reservoir. E_v denotes the valence-band maximum, which we set as the zero of $E_{\rm F}$.

The chemical potentials $\{\mu_\alpha\}$ need to satisfy a set of conditions set out to avoid unwanted competing reactions. For example, we set μ_α^0 to the total energy E_α of elemental solid for $\alpha=$Cu, In, or Ga, and Se, so that

$$\mu_\alpha \leqslant 0. \tag{3}$$

This is so because the host system S would otherwise decompose into its elemental constituents Cu, In, or Ga, and Se. For hydrogen, $\mu_{\rm H}^0$ is set to either to the energy $E({\rm H})$ of free H atom or to half of the total energy $E({\rm H}_2)$ of free H_2 molecule, depending on the external hydrogen source. Moreover, $\mu_{\rm Cu}+\mu_{\rm III}+2\mu_{\rm Se}$ must be equal to to the heat of formation ΔH_f of solid $CuIIISe_2$ if chemical equilibrium is maintained between the host compound and the atomic reservoirs, i.e., $CuIIISe_2(s) \leftrightarrow Cu(s)+III(s)+2Se(s)$. Hence, $\mu_{\rm Cu}+\mu_{\rm III}+2\mu_{\rm Se}=\Delta H_f({\rm CuIIISe_2})$. The latter implies

$$\mu_{\rm Cu},\ \mu_{\rm III},\ 2\mu_{\rm Se} \geqslant \Delta H_f({\rm CuIIISe_2}). \tag{4}$$

The equality in Eq. (3) [Eq. (4)] holds for element α if the the host system is in an environment that is extremely rich [poor] in element α. For example, Cu-rich condition implies $\mu_{\rm Cu}=0$, whereas Cu-poor condition means $\mu_{\rm Cu}=\Delta H_f({\rm CuIIISe_2})$. In addition to Eqs. (3) and (4), we must limit the chemical potentials so that the competing binary phases, such as III_2Se_3 and Cu_2Se, do not form out of $CuIIISe_2$.

The heat of formation used in Eq. (4) as well as the total energies used in Eqs. (1)–(3) were calculated in the framework of the density-functional theory within the local-density approximation (LDA) employing the Ceperley-Alder exchange correlation potential[16] as parametrized by Perdew and Zunger.[17] We utilized the plane-wave total-energy method as implemented in VASP code,[18] and used approximately cubic supercells with fully relaxed atomic positions including 16 molecular units of Cu(In,Ga)Se_2 when no defect is present. We sampled the supercell Brillouin zones by a $2\times2\times2$ **k**-point mesh generated according to the Monkhorst-Pack scheme.[19] The hydrogen (s^1), copper ($d^{10}p^1$), indium (s^2p^1), gallium (s^2p^1), and selenium (s^2p^4) atoms were modeled using ultrasoft pseudopotentials.[20] The plane-wave basis sets were determined by imposing a kinetic-energy cutoff of 234 eV. The electronic self-consistency loop was iterated until the residual convergence error becomes smaller than 0.1 meV, and the atomic positions are relaxed until the error in the total energy (of $\geqslant$64 atoms) becomes smaller than 1 meV. Neutralizing jellium background was added to charged supercells, and the total energy was corrected to $O(L^{-5})$, where L is the supercell size.[21]

These computational settings yield an accurate description of the chalcopyrite lattice for $CuInSe_2$ and $CuGaSe_2$: The equilibrium lattice (a and c) and internal (u) parameters of $CuInSe_2$ are determined as $a=5.701$ and $c=11.464$ Å, and $u=0.2168$ compared to experimental values[22] of $a=5.781$ and $c=11.609$ Å, and $u=0.2281$, respectively, and those of $CuGaSe_2$ are determined as $a=5.513$ and $c=10.941$ Å, and $u=0.2430$ compared to experimental values[23] of $a=5.596$ and $c=11.004$ Å, and $u=0.2423$, respectively. The calculated heat of formations of $CuInSe_2$ and $CuGaSe_2$ are 1.73 and 1.99 eV, respectively, using the calculated cohesive energies: 16.49 eV for $CuInSe_2$, 17.06 eV for $CuGaSe_2$, 4.55 eV for Cu (fcc), 3.11 eV for In (tetragonal), 4.60 eV for Ga (orthorhombic), and 3.55 eV for Se (trigonal). The calculated binding energy (per atom) of H_2 molecule is -2.44 eV, not including the zero-point energy, compared to the experimental value[24] of -2.24 eV. The cohesive and binding energies are calculated with respect to spin polarized free atoms in their ground-state electronic configuration. The spin-polarized energies of free atoms are -0.89, -0.20, -0.12, -0.14, and -0.61 eV for H, Cu, In, Ga, and Se, respectively, within the LDA. The estimated experimental values[25] for heat of formations are 2.11 and 3.27 eV for $CuInSe_2$ and $CuGaSe_2$, respectively, and the experimental cohesive energies[26] are 3.49, 2.81, 2.52, and 2.46 eV for Cu, Ga, In, and Se, respectively. It is not unusual that the LDA overestimates the cohesive energy by 0.5–1.5 eV per atom but the formation energies (which do not involve free-atom quantities) are normally much better.[27] However, the difference between the calculated and experimental heats of formation for $CuGaSe_2$ is unexpectedly large. In this work, we used the calculated total energies because the accumulated error in $[E_D^{(q)}-E_S+\Sigma_\alpha n_\alpha \mu_\alpha^0 - n_{\rm H}\mu_{\rm H}^0]$ in Eq. (2) will be of the same order as the error in the heat of formation. The large error in the cohesive energy, on the other hand, is not transferred to the defect formation energy due to error cancellation between $[E_D^{(q)}-E_S]$ and $[\Sigma_\alpha n_\alpha \mu_\alpha^0 - n_{\rm H}\mu_{\rm H}^0]$ in Eq. (2).

As illustrated for the intrinsic defects in $CuInSe_2$ (Ref. 15) and for H in oxides,[7] the LDA-formation and -transition energies need to be corrected for the LDA band-gap error $\Delta E_g=\Delta E_g^{exp}-E_g^{lda}$. For $CuInSe_2$ LDA calculation results in a near zero band gap, compared to the experimental value[28] of 1.04 eV. The calculated band gap of $CuGaSe_2$ is 0.25 eV, still much smaller than the experimental value[29] of 1.71 eV. For this reason, we developed a correction scheme described in the Appendix. In this scheme, we first shift the LDA-calculated conduction bands so that the band gap is adjusted to its experimental value. We then add the following corrections to the acceptor ($-/0$), direct ($+/-$), and donor ($+/0$) transition energies, respectively,

$$E_{\mathrm{H}}(-/0)=E_{\mathrm{H}}^{lda}(-/0)+[1-C(-/0)][E_g^{exp}-E_g^{lda}], \quad (5)$$

$$E_{\mathrm{H}}(+/-)=E_{\mathrm{H}}^{lda}(+/-)+\frac{1}{2}[1-C(-/0)+C(+/-)][E_g^{exp}-E_g^{lda}],$$

$$E_{\mathrm{H}}(+/0)=E_{\mathrm{H}}^{lda}(+/0)+C(+/0)[E_g^{exp}-E_g^{lda}],$$

where $C(-/0)=0.78$ and $C(+/0)=0.67$ are derived in the Appendix.

III. RESULTS

We carried out first-principles calculations for the following H-involving defects: nonsubstitutionally incorporated hydrogen H_i, substitutional hydrogen on Cu site (H_{Cu}), hydrogen incorporated next to the copper vacancy ($V_{Cu}+H$), and hydrogen incorporated next to the complex formed by an indium or gallium antisite plus two copper vacancies ($III_{Cu}+2V_{Cu}+H$).

A. Location of hydrogen impurity in chalcopyrite lattice

We determined the equilibrium geometries of these defects by minimizing the total energy with respect to atomic positions.

1. H in stoichiometric $Cu(In,Ga)Se_2$

We examined 12 possible sites for hydrogen along the bond directions (i.e., [112] of chalcopyrite lattice), as shown in Fig. 1(a). If Cu is at (0,0,0) and Se at (u, u, 1/2), then the site 3 is called "tetrahedral interstitial" (T), whereas site 2 (closer to Se than T) is called "antibonding" (AB) site. We performed geometry optimizations for H^+, H^0, and H^- initially placed on these 12 sites. We found that H^+ takes up equilibrium position at the Cu-Se bond-center site, as shown in Fig. 1(b). In this atomic configuration, H^+ is closer to the Se atom, at a distance of 1.56 Å from it. Both H^0 [Fig. 1(c)] and H^- [Fig. 1(d)], on the other hand, take up equilibrium position at the tetrahedral site next to In or Ga. However, H^0 attracts the nearest Cu atom strongly towards itself, and cause breaking of a Cu-Se bond whereas H^- find equilibrium at a distance of 1.95 Å from In or Ga, without any significant change in the local host environment. Thus, H^0 is closer to Cu at a distance of 1.69 Å, despite being at the tetrahedral site next to In or Ga, while H^- is closer to In or Ga.

2. H next to V_{Cu}

If H^+ is placed next to V_{Cu}^0 or V_{Cu}^-, it finds its equilibrium position almost at the same location as bond-centered H^+ in perfect $Cu(In,Ga)Se_2$, but now at distance of 1.51 Å from the Se atom. We find that this is the atomic configuration for the ($V_{Cu}+H$) complex when the charge state is *neutral* or +. If the charge state of ($V_{Cu}+H$) is −, however, H is pushed to a distance of 1.76 Å from the Se atom.

3. H next to ($III_{Cu}+2V_{Cu}$)

The defect complex ($III_{Cu}+2V_{Cu}$) includes two copper vacancies that are fcc nearest neighbors of the III_{Cu} antisite, and fcc third neighbors of each other. The location of H in $(III_{Cu}+2V_{Cu}+H)^q$ is practically the same as that in (V_{Cu} +H) in the respective charge states ($q=+,0,-$). This is because H in ($III_{Cu}+2V_{Cu}+H$) interacts with one of the V_{Cu} and the neighboring Se atom so stronger that it does not "see" the other V_{Cu} or III_{Cu}.

4. Comparison of calculated and observed lattice location of hydrogen

Muon implantation into $CuInSe_2$ and subsequent μSR measurements suggest[30,31] that the muon Mu^+ takes up the antibonding site next to Se (AB_{Se}) at low temperatures (below 150 K). This suggestion was based on a comparison between the measured values for the muon depolarization rate to those values calculated within a model.[30] This location for Mu^+ is different from what we calculate for H^+ in $CuInSe_2$, being at the Cu-Se bond center $BC_{Cu\text{-}Se}$ site, at distance of 1.56 Å from the Se atom in stoichiometric material, or at a distance of 1.51 Å from the Se atom if V_{Cu} is present. It could be that the experimental observation[30] corresponds to the latter predicted geometry of H-Se (with bond length of 1.51 Å) around V_{Cu}. But this is likely the case for Mu^+ only at high temperatures since muons implanted into $CuInSe_2$ are trapped by copper vacancies at high temperatures (260–340 K).[31] Our calculations exclude the possibility of AB_{Se} site: H^+ initially placed at AB_{Se} site leads to lattice relaxations, moving towards $BC_{Cu\text{-}Se}$ site, and finally resides at $BC_{Cu\text{-}Se}$. Such relaxation effects were ignored in the model used in Ref. 30 for the interpretation of the μSR data. Hence, the difference between our assignment of $BC_{Cu\text{-}Se}$ site and the assignment[30] of AB_{Se} site could originate from the relaxation effects that might be attributed to the large isotopic mass ratio of hydrogen to muon. We think that our assignment of $BC_{Cu\text{-}Se}$ as the equilibrium position for H^+ is more likely than that inferred[30] from muon implantation experiments.

5. Systematics of hydrogen location in different solids

Table I summarizes[32–35] the calculated equilibrium position of H in different adamantine compounds. We see that with the exception of GaN:H^+ (Ref. 34), the proton H^+ takes up bond-center positions in all cases. In chalcopyrite, there is a choice between Cu-Se and (Ga,In)-Se bonds; H^+ takes up the less electronegative Cu-Se bond. Similarly, the anion H^- takes up in all cases the tetrahedral interstitial site next to the cation. In chalcopyrite, there is a choice between the cations Cu or Ga, In; the anion H^- takes up the tetrahedral site next to the less electronegative (Ga, In). Interestingly, the neutral H^0 reveals a transition from the lattice site location akin to H^+ (BC site) and to the lattice site location akin to H^- (T_{cat} site) with increasing electronegativity difference of the two host elements. For example, H^0 takes up the BC site in Si (electronegativity difference $\Delta\chi=0$), GaAs ($\Delta\chi=0.37$), and Zn(S,Se,Te) ($\Delta\chi=0.45$–0.93), but in the

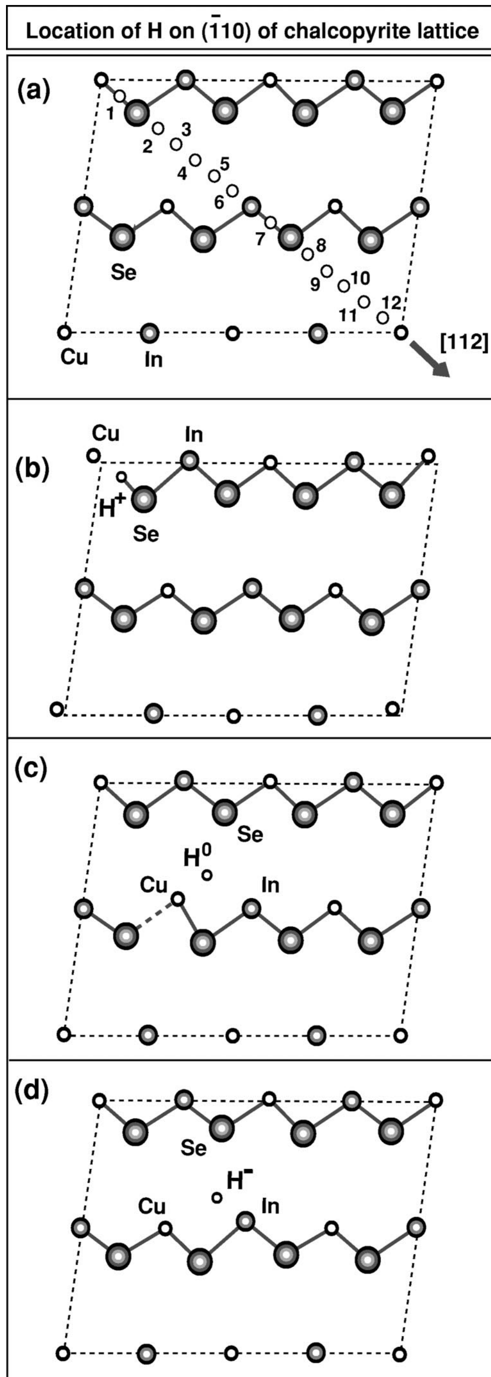

FIG. 1. (a) The possible sites for H in chalcopyrite lattice, along the bond direction, i.e., [112]. The numbered empty circles show (1) the Cu-Se bond-center site at (1/16,1/16,1/16), (2) antibonding site next to Se at (3/16,3/16,3/16), (3) tetrahedral site next to Se at (4/16,4/16,4/16), (4) hexagonal site at (5/16,5/16,5/16), (5) tetrahedral site next to In at (6/16,6/16,6/16), (6) antibonding site next to In at (7/16,7/16,7/16), (7) In-Se bond-center site at (9/16,9/16,9/16), (8) antibonding site next to Se at (11/16,11/16,11/16), (9) tetrahedral site next to Se at (12/16,12/16,12/16), (10) hexagonal site at (13/16,13/16,13/16), (11) tetrahedral site next to Cu at (14/16,14/16,14/16), and (12) antibonding site next to Cu at (15/16,15/16,15/16), putting Cu atom at (0,0,0). (b–d) The equilibrium location of H^+ (b), H^0 (c), and H^- (d) in $Cu(In,Ga)Se_2$.

more electronegative compounds Mg(S,Se,Te) ($\Delta\chi = 0.79$–1.27) and GaN ($\Delta\chi = 1.23$), H^0 takes up the tetrahedral site next to the cation, just as H^- does. In chalcopyrite, there is a choice between the cations Cu or (Ga, In); the neutral H^0 takes up the tetrahedral site next to the less electronegative (Ga, In). In this case, however, H^0 differs from H^- in attracting the closest Cu atom towards itself.

B. Defect formation and transition energies

We calculated the defect formation and transition energies for H_i, H_{Cu}, $(V_{Cu}+H)$, and $(III_{Cu}+2V_{Cu}+H)$. Whereas formation energies [Eq. (2)] depend on chemical potentials, transition energies [Eq. (1)] do not. The explicit dependence of the defect formation energies on the atomic chemical potentials as well as the Fermi energy [cf. Eq. (2)] is shown in Tables II and III where the defect formation energies of hydrogen-involving defects are listed. These formation energies are plotted in Fig. 2 for $CuInSe_2$ as a function of Fermi energy. We fix μ_{Cu}, μ_{In}, and μ_{Se} so that we mimic the growth conditions of *p*-type (In-rich and Cu-poor) $CuInSe_2$ samples used in hydrogenation experiments:[9,10] (i) We set $\mu_{Se}=0$ since chemically pure *p*-type $CuInSe_2$ grows under Se-rich condition.[13] (ii) It has been shown[15] that under In-rich and Cu-poor conditions, ordered arrays of $(In_{Cu}+2V_{Cu})$ complex form spontaneously, so that $CuInSe_2$ (α phase) transforms to other structural phases such as $CuIn_3Se_5$ (β phase) and $CuIn_5Se_8$ (γ phase). Thus, we consider an chemical equilibrium of $CuInSe_2+(In_{Cu}+2V_{Cu})\leftrightarrow CuIn_5Se_8$ to mimic In-rich and Cu-poor conditions. It follows, from points (i) and (ii), $\mu_{In}+\mu_{Cu}=\Delta H_f(CuInSe_2)$ and $\mu_{In}-3\mu_{Cu}=\Delta H_f(CuInSe_2)-\Delta H_f(CuIn_5Se_8)$, respectively, where $\Delta H_f(CuIn_5Se_8)=-7.1$ eV within the LDA. The values of μ_{In} and μ_{Cu} are then obtained by solving the latter two equations simultaneously. For μ_H, we consider equilibrium in atomic H-rich environment so that $\mu_H=E(H)$. This is shown by the vertical scale on the left-hand side in Fig. 2. One could, instead, also imagine equilibrium in molecular H_2-rich environment so that $\mu_H=(1/2)E(H_2)$. The vertical scale on the right-hand side in Fig. 1 shows this case. The defect transition energies are marked by filled circles, and the charge states are as indicated.

It is seen in Fig. 2 that the charge state transition occurs *directly* from $q=+$ to $q=-$ for both H_i and $(III_{Cu}+2V_{Cu}+H)$, showing that these defects do not become *neutral* for any value of Fermi energy. The latter is the case for hydrogen in most semiconductors,[1] and is known as the *negative-U* behavior.[7] This means that hydrogen will act as a shallow donor or acceptor if its direct $(+/-)$ transition level is in the vicinity of the conduction-band minimum (CBM) or valence-band maximum (VBM), respectively. Figure 2 shows that the direct $(+/-)$ transition level of H_i is located at $E_c-0.39$ eV in $CuInSe_2$, where E_c denotes the conduction-band minimum, i.e., nonsubstitutionally incorporated hydrogen forms a rather deep donor. On the other hand, nonstoichiometric $CuInSe_2$ contains $(In_{Cu}+2V_{Cu})$ defect complex.[15] The direct transition level of $(III_{Cu}+2V_{Cu}+H)$ is located at $E_c-0.15$ eV in $CuInSe_2$. Thus, the incorporation

TABLE I. The equilibrium locations of H^+, H^0, and H^- (columns II–IV, respectively) in various systems in diamond [Si (Ref. 32)], zinc blende [GaAs (Ref. 33), GaN (Ref. 34), (Mg,Zn) (S,Se,Te) (Ref. 35)], and chalcopyrite [$Cu(In,Ga)Se_2$] structures. $BC_{\alpha\text{-}\beta}$, T_α, and AB_α denote the bond-center site between two atoms α and β, the tetrahedral site next to α, and the antibonding site next to α, respectively. The atomic electronegativities χ on Pauling scale are given in column V. $\chi_H = 2.20$ for comparison.

System	H^+	H^0	H^-	Electronegativity
Si	$BC_{Si\text{-}Si}$	$BC_{Si\text{-}Si}$	T_{Si}	$\chi_{Si}=1.90$
GaAs	$BC_{Ga\text{-}As}$	$BC_{Ga\text{-}As}$	T_{Ga}	$\chi_{Ga}=1.81$; $\chi_{As}=2.18$
ZnVI (VI=S,Se,Te)	$BC_{Zn\text{-}VI}$	$BC_{Zn\text{-}VI}$	T_{Zn}	$\chi_{Zn}=1.65$; $\chi_{S,Se,Te}=2.58,2.55,2.10$
MgVI (VI=S,Se,Te)	$BC_{Mg\text{-}VI}$	T_{Mg}	T_{Mg}	$\chi_{Mg}=1.31$; $\chi_{S,Se,Te}=2.58,2.55,2.10$
$CuIIISe_2$ (III=In,Ga)	$BC_{Cu\text{-}Se}$	T_{III}	T_{III}	$\chi_{Cu}=1.90$; $\chi_{In,Ga}=1.78,1.81$; $\chi_{Se}=2.55$
GaN	AB_N	T_{Ga}	T_{Ga}	$\chi_{Ga}=1.81$; $\chi_N=3.04$

of H next to $(III_{Cu}+2V_{Cu})$ results in a shallow electrical level. This is due to the fact that $(III^{2+}_{Cu}+2V^-_{Cu})^0$ has two negatively charged copper vacancies and the incorporated hydrogen being next to V^-_{Cu} prefers to be in + charge state as opposed to − charge state owing to electrostatic interaction. The latter implies a *positive* contribution to the direct transition energy so that $E_{In_{Cu}+2V_{Cu}+H}(+/-)=E_{H_i}(+/-)+0.24$ eV.

Hydrogenation of $CuInSe_2$ was observed to pin the Fermi level at $E_c-(0.1\pm0.1)$ eV (Refs. 9 and 36), converting the material n type. We explain this by the calculated donor level of $(In+2V_{Cu}+H)$ at $E_c-0.15$ eV, showing that hydrogen dopes n type $CuInSe_2$ owing to the formation of $(In+2V_{Cu}+H)^+$. Thus, the observed[9,10,36] conductivity-type conversion in $CuInSe_2$ is explained.

Figure 2 also shows that the defects H_{Cu} and $(V_{Cu}+H)$ are *neutral* for $E_v\leqslant E_F\leqslant E_c$. This implies that the negatively charged copper vacancies will be passivated upon incorporation of hydrogen *once* these defects form. Thus, p-type electrical conduction will be weakened upon hydrogenation because the electrons released as a result of H^+ formation will compensate the holes promoted by V^-_{Cu}. The effect of hydrogen incorporation on the electrical properties of $Cu(In,Ga)Se_2$ can then be considered as an interplay between *passivation* and *n-type doping*, cf. Sec. III D below.

Figure 3 summarizes the calculated electrical levels, i.e., the hydrogen transition energies, in $CuInSe_2$ and $CuGaSe_2$. It is seen that hydrogen electrical levels in $CuGaSe_2$ are ~0.2 eV deeper relative to $CuInSe_2$. Thus, n-type doping by hydrogen will be much *less* effective in $CuGaSe_2$ compared to $CuInSe_2$. The fact that the CBM of $CuGaSe_2$ is ~0.6 eV above that of $CuInSe_2$ (Ref. 37) explains why hydrogen forms a deeper donor level in the former and a relatively shallow level in the latter.

C. The role of H source and the internal H reservoir

We see in Fig. 2 that the formation energies of H-involving defects are *negative* (cf. the vertical scale on the left), in equilibrium with *atomic* H source, whereas they are *positive* (cf. the vertical scale on the right), in equilibrium with *molecular* H_2 source. Thus, hydrogen incorporation from atomic H source into $Cu(In,Ga)Se_2$ is *exothermic*, tak-

TABLE II. The defect formation energies for hydrogen-involving defects in $CuInSe_2$ as a function of μ_α and E_F. The zeros of μ_H, μ_{Cu}, μ_{In}, and E_F are set to the energy of H atom, the total energy of Cu solid, the total energy of In solid, and the valence-band maximum of $CuInSe_2$, respectively.

Defect	Formation energy (eV)
H_i^+	$-1.68-\mu_H+E_F$
H_i^0	$-0.50-\mu_H$
H_i^-	$-0.21-\mu_H-E_F$
H_{Cu}^+	$-0.94-\mu_H+\mu_{Cu}+E_F$
H_{Cu}^0	$-1.29-\mu_H+\mu_{Cu}$
H_{Cu}^-	$0.18-\mu_H+\mu_{Cu}-E_F$
$(V_{Cu}+H)^+$	$-1.59-\mu_H+\mu_{Cu}+E_F$
$(V_{Cu}+H)^0$	$-1.93-\mu_H+\mu_{Cu}$
$(V_{Cu}+H)^-$	$-0.33-\mu_H+\mu_{Cu}-E_F$
$(In_{Cu}+2V_{Cu}+H)^+$	$-1.57-\mu_H+3\mu_{Cu}-\mu_{In}+E_F$
$(In_{Cu}+2V_{Cu}+H)^0$	$-0.33-\mu_H+3\mu_{Cu}-\mu_{In}$
$(In_{Cu}+2V_{Cu}+H)^-$	$0.26-\mu_H+3\mu_{Cu}-\mu_{In}-E_F$

TABLE III. The defect formation energies for hydrogen-involving defects in $CuGaSe_2$ as a function of μ_α and E_F. The zeros of μ_H, μ_{Cu}, μ_{Ga}, and E_F are set to the energy of H atom, the total energy of Cu solid, the total energy of Ga solid, and the valence-band maximum of $CuGaSe_2$, respectively.

Defect	Formation energy (eV)
H_i^+	$-1.33-\mu_H+E_F$
H_i^0	$-0.19-\mu_H$
H_i^-	$0.03-\mu_H-E_F$
H_{Cu}^+	$-0.66-\mu_H+\mu_{Cu}+E_F$
H_{Cu}^0	$-1.34-\mu_H+\mu_{Cu}$
H_{Cu}^-	$0.42-\mu_H+\mu_{Cu}-E_F$
$(V_{Cu}+H)^+$	$-1.30-\mu_H+\mu_{Cu}+E_F$
$(V_{Cu}+H)^0$	$-1.98-\mu_H+\mu_{Cu}$
$(V_{Cu}+H)^-$	$-0.11-\mu_H+\mu_{Cu}-E_F$
$(Ga_{Cu}+2V_{Cu}+H)^+$	$-1.68-\mu_H+3\mu_{Cu}-\mu_{Ga}+E_F$
$(Ga_{Cu}+2V_{Cu}+H)^0$	$-0.32-\mu_H+3\mu_{Cu}-\mu_{Ga}$
$(Ga_{Cu}+2V_{Cu}+H)^-$	$0.17-\mu_H+3\mu_{Cu}-\mu_{Ga}-E_F$

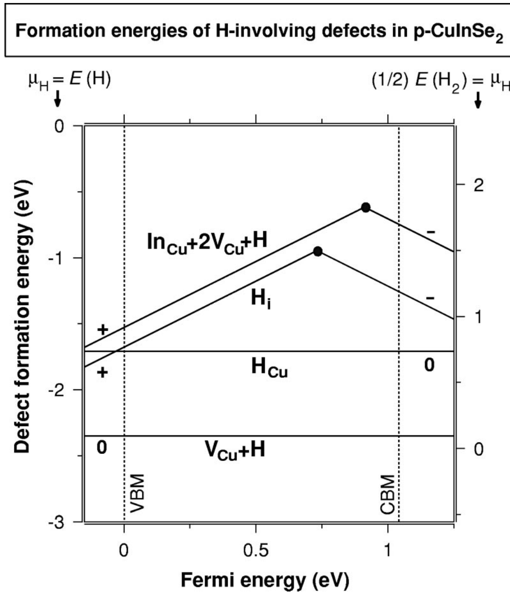

FIG. 2. The LDA-corrected formation energies of H_i, H_{Cu}, $(V_{Cu}+H)$, and $(In_{Cu}+2V_{Cu}+H)$ in $CuInSe_2$ as a function of the Fermi energy E_F for Cu-poor, In-rich, and Se-rich conditions. Two different hydrogen sources are considered: atomic H (left scale) or molecular H_2 (right scale). The zero of E_F is set to the valence-band maximum. $+$, 0, and $-$ denote the charge states. The transition energies are marked by filled circles.

ing place spontaneously, whereas incorporation from H_2 is *endothermic*. This explains the experimental difficulty[38] with H incorporation from H_2 gas, and verifies that the use of atomic hydrogen is crucial.[38] We find in the latter case that the implanted hydrogen atoms can decorate copper vacancies inside $Cu(In,Ga)Se_2$, causing formation of an *internal hydrogen reservoir*. To explain this point, we first consider the decoration of a defect D by a number m of H atoms or H_2 molecules. The resulting defect complex is denoted as $D+mH_n$, where $n=1$ and 2 for atomic and molecular hydrogen, respectively. The change in energy upon incorporation of m H_n species into $S=Cu(In,Ga)Se_2$ next to defect D is *termed* as the *hydrogen incorporation energy*, given by

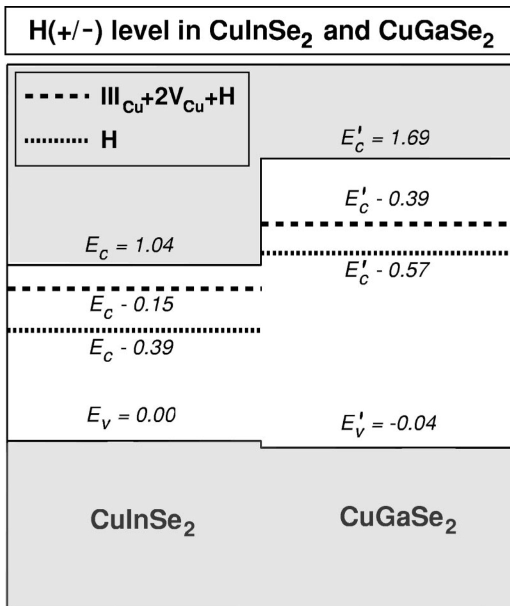

FIG. 3. The electrical hydrogen level in $CuInSe_2$ and $CuGaSe_2$. LDA-calculated valence-band offset (Ref. 37) is used to put VBMs of $CuInSe_2$ and $CuGaSe_2$ on the same energy scale in eV.

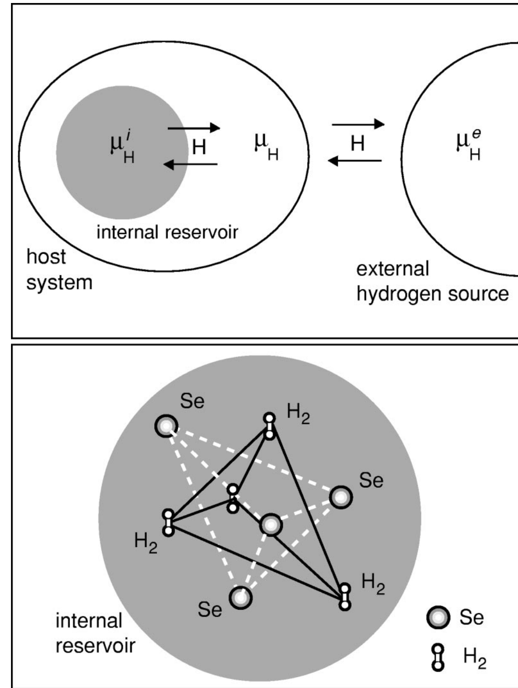

FIG. 4. The formation of an internal H reservoir is schematically shown (top). The corresponding atomic configuration is illustrated (bottom) for the internal reservoir formed by *four* H_2 molecules at the corners of the V_{Cu}-centered tetrahedron. The tetrahedron (white dashed lines) formed by Se atoms also centered about V_{Cu} is orthogonal to the H_2 tetrahedron.

$$\Delta E_D^{(m,n)} = E_{D+mH_n}^{(0)} - E_D^{(0)} - mn(\mu_H + \mu_H^0), \tag{6}$$

where the zero of hydrogen chemical potential is set to the energy of H atom, i.e., $\mu_H^0 = E(H)$. We first note that $D+mH_n$ forms spontaneously if $\Delta E_D^{(m,n)}$ is *negative*. We next consider incorporation of hydrogen into the host system S from some external hydrogen source. The top panel of Fig. 4 shows this situation schematically. The external hydrogen source (with chemical potential μ_H^e) pumps H into the system S if $\mu_H \leqslant \mu_H^e$ (otherwise hydrogen would leave the system S, diffusing into the source). Similarly, hydrogen species (with chemical potential μ_H^i) decorating defect D form an internal reservoir when $\mu_H \leqslant \mu_H^i$. Since $E_{D+mH_n}^0 - E_D^0$ in Eq. (6) corresponds to the change in the internal energy upon incorporation of m H_n species next to D, the incorporation energy is proportional to $\mu_H^i - \mu_H$. It follows then that hydrogen species decorating D act as an internal reservoir if the value of μ_H is so that $\Delta E_D^{m,n}$ is *positive*.

Figure 5 shows the hydrogen incorporation energy with respect to the hydrogen chemical potential for various *neu-*

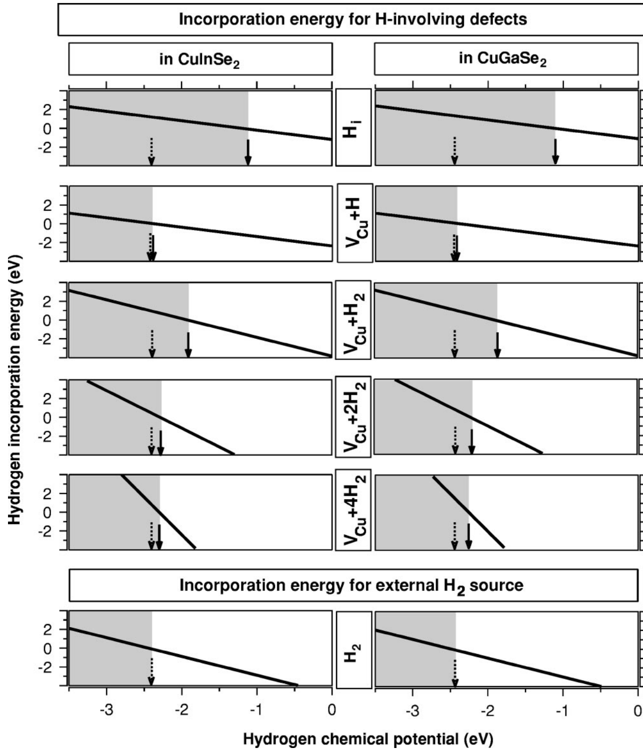

FIG. 5. The hydrogen incorporation energies $\Delta E_D^{m,n}$ [given in Eq. (6)] for H_i, $V_{Cu}+H$, $V_{Cu}+H_2$, $V_{Cu}+2H_2$, and $V_{Cu}+4H_2$ in $CuInSe_2$ (left) and $CuGaSe_2$ (right) with respect to the hydrogen chemical potential μ_H. The zero of μ_H is set to the energy of H atom. The incorporation energy for the external reservoir of H_2 is also shown in the bottom panels, for comparison. The shaded area represents where $\Delta E_D^{m,n} \geqslant 0$. The solid arrows locate $\mu_H^*(D+mH_n)$, i.e., the value of μ_H for which $\Delta E_D^{m,n}=0$, on the horizontal axis while the dotted arrows locate $\mu_H^*(H_2)$.

tral H-involving defects: H_i, $(V_{Cu}+H)$, $(V_{Cu}+H_2)$, $(V_{Cu}+2H_2)$, and $(V_{Cu}+4H_2)$. The incorporation energy for the external reservoir of H_2 is shown in the bottom panels for comparison. It is seen that $\Delta E_D^{m,n}$ can be positive or negative, depending on the value of μ_H. Hence, the range of μ_H is divided into two regions, as indicated by shading in Fig. 5, for each $D+mH_n$: (i) $\mu_H^*(D+mH_n)<\mu_H$ and (ii) $\mu_H<\mu_H^*(D+mH_n)$, where $\mu_H^*(D+mH_n)$ denotes the value of μ_H for which $\Delta E_D^{m,n}=0$. For external reservoir of H_2, $\mu_H^*(H_2)=E(H_2)$ due to the fact that the elemental ground state of hydrogen is H_2. If μ_H has a value within region (i), then $\Delta E_D^{(m,n)}<0$, so that decoration of D by m H_n species takes place spontaneously. On the other hand, if μ_H has a value within region (ii), then $D+mH_n$ acts an internal reservoir since $\Delta E_D^{(m,n)}>0$. Thus, the internal hydrogen reservoir forms in two stages characterized by the value of μ_H: The first stage involves spontaneous decoration of D by m H_n species [i.e., μ_H adjusted to some value within region (i) as in, e.g., implantation experiments[9,10,36,38]] so that a significant amount of hydrogens is incorporated. In the second stage, the subsequent relaxation of the system following the implantation make μ_H decrease to some value within region (ii), so that $D+mH_n$ acts as a reservoir. In this process, increasing the value of μ_H in the first stage is crucial since the second stage consists only of uncontrolled relaxations.

According to Fig. 5, implanted hydrogens form H_i spontaneously if $\mu_H \geqslant \mu_H^*(H_i)$, where

$$\mu_H^*(H_i)=\mu_H^*(H_2)+1.25[1.32]\ \text{eV}$$

for $CuInSe_2$ [$CuGaSe_2$]. The difference $\mu_H^*(H_i)-\mu_H^*(H_2)$ measures the increase in μ_H with respect to the equilibrium value of μ_H in the external reservoir of H_2. Since the latter is larger than 1 eV (per implanted H atom), it is hardly expected for μ_H to pin $\mu_H^*(H_i)$ without damaging the host system. For $(V_{Cu}+H)$, on the other hand, we have

$$\mu_H^*(V_{Cu}+H)=\mu_H^*(H_2)+0.07[0.10]\ \text{eV}$$

for $CuInSe_2$ [$CuGaSe_2$]. Thus, the difference $\mu_H^*(D+mH_n)-\mu_H^*(H_2)$ for $(V_{Cu}+H)$ is smaller by more than an order of magnitude in comparison to that for H_i. This shows that decoration of V_{Cu} requires a small increase in μ_H, with respect to the equilibrium value of μ_H in the external reservoir H_2, which could be supplied during the implantation process without damaging the host system. For the m H_n species decorating V_{Cu}, we have

$$\mu_H^*(V_{Cu}+H_2)=\mu_H^*(H_2)+0.52[0.60]\ \text{eV},$$

$$\mu_H^*(V_{Cu}+2H_2)=\mu_H^*(H_2)+0.16[0.25]\ \text{eV},$$

$$\mu_H^*(V_{Cu}+4H_2)=\mu_H^*(H_2)+0.14[0.23]\ \text{eV}$$

for $CuInSe_2$ [$CuGaSe_2$]. In addition, we have

$$\mu_H^*(\text{CuIIISe}_2{:}H_2)=\mu_H^*(H_2)+0.23[0.33]\ \text{eV},$$

$$\mu_H^*(\text{CuIIISe}_2{:}2H_2)=\mu_H^*(H_2)+0.17[0.27]\ \text{eV},$$

$$\mu_H^*(\text{CuIIISe}_2{:}4H_2)=\mu_H^*(H_2)+0.17[0.27]\ \text{eV}$$

for the H_2 molecules accumulated around Cu atom in stoichiometric regions of $CuInSe_2$ [$CuGaSe_2$]. Hence, decoration of V_{Cu} by two or four H_2 molecules as well as accumulation of one, two, or four H_2 molecules around Cu also requires a relatively small increase in μ_H with respect to the equilibrium value of μ_H in the external reservoir H_2. Thus, implanted hydrogens either accumulate around copper atoms or decorate copper vacancies. In the latter case, $(V_{Cu}+H)$, $(V_{Cu}+2H_2)$, and $(V_{Cu}+4H_2)$ are formed, resulting in an internal H reservoir. This is illustrated for $(V_{Cu}+4H_2)$ in the bottom panel of Fig. 4, where *four* H_2 molecules form a tetrahedron orthogonal to that of Se atoms neighboring V_{Cu}. This reservoir supplies hydrogens to form the electrically active H-involving defects. As the system is equilibrated for a long enough period under some H-poor atmosphere (e.g., air), μ_H gets eventually smaller than $\mu_H^*(V_{Cu}+mH_n)$, so hydrogen tends to diffuse out until μ_H pins to the equilibrium value of μ_H in H-poor atmosphere. This prediction is in line with the observation that[36] the p-to-n conversion is reversed if the sample is stored in air. Thus, the hydrogen implanted into $Cu(In,Ga)Se_2$ can be taken out by adjusting the external

TABLE IV. The enthalpies (in eV) of defect-pairing reactions in $CuInSe_2$ and $CuGaSe_2$. There is no dependence on the atomic chemical potentials or the Fermi energy since the pairing reactions are atom and charge balanced.

Reaction	$CuInSe_2$	$CuGaSe_2$
$V_{Cu}^{-}+H_i^{+}\rightarrow H_{Cu}^{0}$	0.32	0.29
$V_{Cu}^{-}+H_i^{+}\rightarrow(V_{Cu}+H)^{0}$	−0.33	−0.35
$(III_{Cu}+2V_{Cu})^{0}+H_i^{+}\rightarrow(III_{Cu}+2V_{Cu}+H)^{+}$	0.00	−0.35
$(III_{Cu}+2V_{Cu})^{0}+H_i^{-}\rightarrow(III_{Cu}+2V_{Cu}+H)^{-}$	0.36	0.14

conditions so that chalcopyrites may be utilized for hydrogen storage. The atomic weight percent of hydrogen, however, seems to be rather low [$\sim$0.2–0.3 % for 10% Cu deficient $Cu(In,Ga)Se_2$] for practical applications.

D. Hydrogen in nonstoichiometric p-$Cu(In,Ga)Se_2$

As we mentioned in Sec. II B, the effect of hydrogen in nonstoichiometric chalcopyrite (i.e., containing V_{Cu} and/or $III_{Cu}+2V_{Cu}$) depends on the interplay between passivation and *n*-type doping. This can be explained in terms of reaction enthalpies for pairing of the defects in $Cu(In,Ga)Se_2$, listed in Table IV. We see that pairing of V_{Cu}^{-} and H_i^{+} to form H_{Cu}^{0} is *endothermic*, whereas it is *exothermic* for forming $(V_{Cu}+H_i)^0$. Thus, hydrogen prefers to reside *next* to copper vacancy, as opposed to substitute the vacant Cu site. In systems where the negatively charged copper vacancies preexist, e.g., in chemically pure *p*-type $Cu(In,Ga)Se_2$, hydrogen will then be incorporated into the $(V_{Cu}+H_i)^0$ defect complex. Since neutral $(V_{Cu}+H_i)^0$ is electrically inactive, hydrogen will thus passivate *p*-type $Cu(In,Ga)Se_2$. Table IV also shows that pairing of H^+ with $(III_{Cu}+2V_{Cu})^0$ to form donorlike $(III_{Cu}+2V_{Cu}+H)^+$ is *exothermic*, whereas that of H^- to form acceptorlike $(III_{Cu}+2V_{Cu}+H)^-$ is *endothermic*. Thus, similar to the case with V_{Cu}^{-}, hydrogen prefers to be incorporated next to $(III_{Cu}+2V_{Cu})^0$. Hence, the incorporation of hydrogen into nonstoichiometric $Cu(In,Ga)Se_2$ and the effect of H on electrical conduction are controlled by the amounts of preexisting intrinsic defects V_{Cu}^{-} and $(III_{Cu}+2V_{Cu})^0$.

IV. SUMMARY

Our first-principles study shows that the main electrical effect of hydrogen incorporation on chalcopyrites can be summarized as an interplay between *n*-type doping and passivation. The former is determined by the location of the chalcopyrite CBM, while the latter is controlled by the interaction with the intrinsic defects, i.e., nonstoichiometry. In this respect, H incorporation leads to *n*-type doping and passivation of acceptorlike defects in $CuInSe_2$, while only passivation of acceptor-like defects in $CuGaSe_2$. This is explained by noting that the CBM of $CuGaSe_2$ is considerably higher than that of $CuInSe_2$. Despite this difference in electrical behavior towards hydrogen, it is illustrated that the hydrogen incorporation (via implantation or otherwise) leads to formation of an internal H reservoir in both $CuInSe_2$ and $CuGaSe_2$.

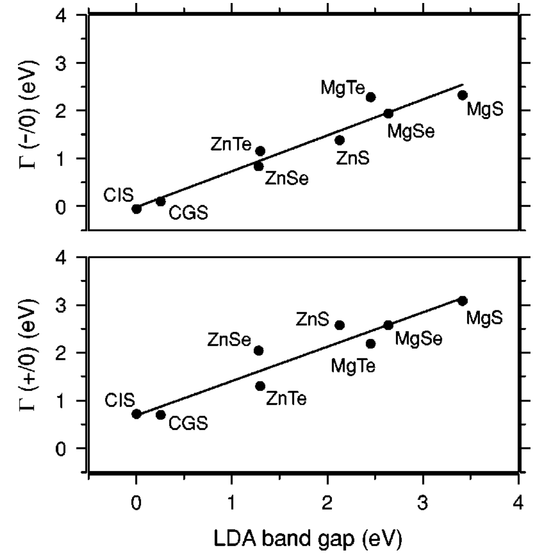

FIG. 6. The LDA-calculated $\Gamma(-/0)=E_c-E_H(-/0)$ (top) and $\Gamma(+/0)=E_H(+/0)-E_v$ (bottom) as a function of the LDA band gap for chalcopyrite $CuInSe_2$ and $CuGaSe_2$, and zinc blende ZnS, ZnSe, ZnTe, MgTe, MgSe, and MgS. The lines show the result of regression analysis summarized in Eq. (A1).

ACKNOWLEDGMENTS

We like to thank to K. Otte, L. G. Wang, J. Abushama, and M. Contreras for useful discussions. This work was supported by the US DOE-SC-BES under Contract No. DE-AC36-99GO10337 and the NERSC for IBM SP time.

APPENDIX: CORRECTING DEFECT TRANSITION ENERGIES FOR LDA BAND-GAP ERROR

Here we introduce a practical scheme for correcting defect transition energies $E(q_1/q_2)$ for the LDA band gap error $\Delta E_g=E_g^{exp}-E_g^{lda}$. The formation energy of a defect $\Delta H_D^{(q)}$ [Eq. (2)] and the transition energy $E_D(q_1/q_2)$ [Eq. (1)] both depend indirectly on the value of the band-gap. In principle, these dependencies can be monitored by causing a real or computational change in the band gap, and monitoring ensuing change in $\Delta H_D^{(q)}$ and $E_D(q_1/q_2)$. In Ref. 39, the cutoff energy $E1$ for the plane-wave basis set was used to alter $E_g^{lda}(E1)$ and $\Delta H_D^{(q)}(E1)$, and the resulting functional relationship was used to extrapolate $\Delta H_D^{(q)}$ to its value when the band gap E_g^{lda} was replaced by the experimental value. Another way to explore the dependence of $E_D(q_1/q_2)$ on E_g is to use chemical identity to alter both.[35] Figure 6 shows the dependence of the distance $\Gamma(-/0)=E_c-E_H(-/0)$ of the acceptor level from the CBM on the band gap for different II-VI-like compounds, and the distance $\Gamma(+/0)=E_H(+/0)-E_v$ of the donor level from the VBM. It is seen that both $\Gamma(-/0)$ and $\Gamma(+/0)$ vary linearly with E_g^{lda}. Thus, we parametrize these quantities within LDA as

$$\Gamma_{lda}(q_1/q_2) = G(q_1/q_2) + C(q_1/q_2)E_g^{lda}, \tag{A1}$$

where $G(q_1/q_2)$ and $C(q_1/q_2)$ denote coefficients determined via regression analysis of Fig. 6: $G(-/0) = -0.04$, $G(+/0) = 0.46$, $C(-/0) = 0.78$, and $C(+/0) = 0.67$, corresponding to rms deviations of 0.20 and 0.24 eV in $\Gamma(-/0)$ and $\Gamma(+/0)$, respectively.

Comparison of the LDA transition energies with the corrected transition energies obtained from previously used band-gap-correction schemes[7,40] indicates that a reasonable description for the variation of $\Gamma(q_1/q_2)$ can, indeed, be obtained within the LDA despite the fact that the LDA involves large error regarding the band gap. We assume that Eq. (A2) should be applicable also for the experimental band gap E_g^{exp}, so that

$$\Gamma(q_1/q_2) = G(q_1/q_2) + C(q_1/q_2)E_g^{exp}. \tag{A2}$$

From Eqs. (A1) and (A2), we obtain

$$\Delta\Gamma(q_1/q_2) = C(q_1/q_2)\Delta E_g, \tag{A3}$$

where $\Delta\Gamma(q_1/q_2) = \Gamma(q_1/q_2) - \Gamma_{lda}(q_1/q_2)$ denotes the correction to $\Gamma(q_1/q_2)$ due to LDA band-gap error, and $\Delta E_g = E_g^{exp} - E_g^{lda}$ is the band-gap error.

The correction to the LDA acceptor $(-/0)$ and donor $(+/0)$ transition energies can now be obtained from Eq. (A3) as

$$\Delta E_{\mathrm{H}}(-/0) = \Delta E_c - C(-/0)\Delta E_g, \tag{A4}$$

$$\Delta E_{\mathrm{H}}(+/0) = \Delta E_v + C(+/0)\Delta E_g,$$

respectively. Here $\Delta E_c = E_c^{exp} - E_c^{lda}$ and $\Delta E_v = E_v^{exp} - E_v^{lda}$ denote the correction for the CBM and VBM, respectively. The correction to the direct $(+/-)$ transition energy is given by

$$\Delta E_{\mathrm{H}}(+/-) = \frac{1}{2}[\Delta E_{\mathrm{H}}(-/0) + \Delta E_{\mathrm{H}}(+/0)], \tag{A5}$$

according to Eq. (1) of Sec. II.

Since $\Delta E_g = \Delta E_c - \Delta E_v$, Eq. (A4) can be rewritten as

$$\Delta E_{\mathrm{H}}(-/0) = C(-/0)\Delta E_v + [1 - C(-/0)]\Delta E_c,$$
$$\Delta E_{\mathrm{H}}(+/0) = C(+/0)\Delta E_c + [1 - C(+/0)]\Delta E_v. \tag{A6}$$

The values of $C(-/0) = 0.78$ and $C(+/0) = 0.67$ in conjunction with this equation indicate that the acceptor $(-/0)$ transition energy follows largely the valence-band edge, whereas the donor $(+/0)$ transition energy follows largely the conduction-band edge. It is interesting to note that the latter was the basic assumption in Ref. 15 to correct the band-gap error for the intrinsic defects in $CuInSe_2$. In the present framework, the band-gap correction in Ref. 15 corresponds to the case where $C(-/0)$ and $C(+/0)$ are *ad hoc* set to unity. Our procedure makes an empirical determination of these coefficients possible, using the *first-principles* data. If we further assume that $\Delta E_g \simeq \Delta E_c$, Eqs. (A5) and (A6) simplify to the Eq. (5) of Sec. II, which we used in practical applications.

[1] S.K. Estreicher, Mater. Sci. Eng. R **14**, 319 (1995).
[2] C.G. Van de Walle, P.J.H. Denteneer, Y. Bar-Yam, and S.T. Pantelides, Phys. Rev. B **39**, 10 791 (1989).
[3] N.M. Johnson, R.D. Burnham, R.A. Street, and R.L. Thornton, Phys. Rev. B **33**, 1102 (1986).
[4] B. Clerjaud, D. Côte, W.-S. Hahn, D. Wasik, and W. Ulrici, Appl. Phys. Lett. **60**, 2374 (1992).
[5] E.M. Omeljanovsky, A.V. Pakhomov, and A.Y. Polyakov, Phys. Lett. A **141**, 75 (1989).
[6] E. Ho, P.A. Fisher, J.L. House, G.S. Petrich, L.A. Kolodziejski, J. Walker, and N.M. Johnson, Appl. Phys. Lett. **66**, 1062 (1995).
[7] Ç. Kılıç and A. Zunger, Appl. Phys. Lett. **81**, 73 (2002).
[8] Ç. Kılıç and A. Zunger, Phys. Rev. Lett. **88**, 095501 (2002).
[9] K. Otte, G. Lippold, D. Hirsh, R.K. Gebhardt, and T. Chassá, Appl. Surf. Sci. **179**, 203 (2001).
[10] K. Yoshino, T. Yamamoto, T. Ikari, M. Yakushev, R.D. Pilkington, and S.F. Chichibu, J. Phys. Chem. Solids (to be published).
[11] J.J. Loferski, Mater. Sci. Eng., B **13**, 271 (1992).
[12] E.I. Rogacheva and T.V. Tavrina, J. Phys. Chem. Solids (to be published).
[13] S. Siebentritt, Thin Solid Films **403-404**, 1 (2002).
[14] R. Noufi, R.C. Powell, and R.J. Matson, Sol. Cells **21**, 55 (1987).
[15] S.B. Zhang, S.-H. Wei, A. Zunger, and H. Katayama-Yoshida, Phys. Rev. B **57**, 9642 (1998).
[16] D.M. Ceperley and B.J. Alder, Phys. Rev. Lett. **45**, 566 (1980).
[17] J.P. Perdew and A. Zunger, Phys. Rev. B **23**, 5048 (1981)
[18] G. Kresse and J. Furthmuller, Comput. Mater. Sci. **6**, 15 (1996).
[19] H.J. Monkhorst and J.D. Pack, Phys. Rev. B **13**, 5188 (1976).
[20] D. Vanderbilt, Phys. Rev. B **41**, 7892 (1990).
[21] G. Makov and M.C. Payne, Phys. Rev. B **51**, 4014 (1995).
[22] G. Zahn and P. Paufler, Cryst. Res. Technol. **23**, 499 (1988).
[23] S.C. Abrahams and J.L. Bernstein, J. Chem. Phys. **61**, 1140 (1974).
[24] B.P. Stoicheff, Can. J. Phys. **79**, 165 (2001).
[25] D. Cahen and R. Noufi, J. Phys. Chem. Solids **52**, 947 (1991).
[26] C. Kittel, *Introduction to Solid State Physics*, 6th ed. (Wiley, New York, 1986).
[27] B. Farid and R.J. Needs, Phys. Rev. B **45**, 1067 (1992).
[28] Ariswan, G. El Haj Moussa, F. Guastavino, and C. Llinares, J. Mater. Sci. Lett. **21**, 215 (2002).
[29] R. Diaz, T. Martin, J.M. Merino, M. Leon, and F. Rueda, J. Vac. Sci. Technol. A **18**, 2957 (2000).
[30] J.M. Gil, P.J. Mendes, L.P. Ferreira, H.V. Alberto, R.C. Vilão, N. Ayres de Campos, A. Weidinger, Y. Tomm, Ch. Niedermayer, M.V. Yakushev, R.D. Tomlinson, S.P. Cottrell, and S.F.J. Cox, Phys. Rev. B **59**, 1912 (1999).
[31] R.C. Vilão, J.M. Gil, H.V. Alberto, J. Piroto Duarte, N. Ayres de

Campos, A. Weidinger, M.V. Yakushev, and S.F.J. Cox, Physica B **326**, 181 (2003).
[32] C. Herring, N.M. Johnson, and C.G. Van de Walle, Phys. Rev. B **64**, 125209 (2001).
[33] C. Wang and Q.-M. Zhang, Phys. Rev. B **59**, 4864 (1999).
[34] J. Neugebauer and C.G. Van de Walle, Phys. Rev. Lett. **75**, 4452 (1995).
[35] Ç. Kılıç, L.-G. Wang, and A. Zunger (unpublished).
[36] K. Otte, T. Chasse, G. Lippold, B. Rauschenbach, and R. Szargan, J. Appl. Phys. **91**, 1624 (2002).
[37] S.B. Zhang, S.-H. Wei, and A. Zunger, J. Appl. Phys. **83**, 3192 (1998).
[38] A. Weidinger, J. Krauser, Th. Riedle, R. Klenk, M.Ch. Lux-Steiner, and M.V. Yakushev, in *Hydrogen in Semiconductors and Metals*, edited by N. H. Nickel, W. B. Jackson, and R. C. Bowman, MRS Symposia Proceedings No. 513 (Materials Research Society, Pittsburgh, 1997), p. 177.
[39] S.B. Zhang, S.-H. Wei, and A. Zunger, Phys. Rev. Lett. **84**, 1232 (2000).
[40] C. Stampfl, C.G. Van de Walle, D. Vogel, P. Krüger, and J. Pollmann, Phys. Rev. B **61**, R7846 (2000).